Langmuir

Letter

pubs.acs.org/Langmuir

Nanopore-Spanning Lipid Bilayers on Silicon Nitride Membranes That Seal and Selectively Transport Ions

Christopher E. Korman,[†] Mischa Megens,[†] Caroline M. Ajo-Franklin,[‡,§] and David A. Horsley*[,†]

[†]Department of Mechanical and Aerospace Engineering, University of California, Davis, California 95616, United States

[‡]Physical Biosciences Division and [§]Materials Science Division, Lawrence Berkeley National Laboratory, Berkeley, California 94720, United States

Supporting Information

ABSTRACT: We report the formation of POPC lipid bilayers that span 130 nm pores in a freestanding silicon nitride film supported on a silicon substrate. These solvent-free lipid membranes self-assemble on organosilane-treated Si_3N_4 via the fusion of 200 nm unilamellar vesicles. Membrane fluidity is verified by fluorescence recovery after photobleaching (FRAP), and membrane resistance in excess of 1 GΩ is demonstrated using electrical impedance spectroscopy (EIS). An array of 40 000 membranes maintained high impedance over 72 h, followed by rupture of most of the membranes by 82 h. Membrane incorporation of gramicidin, a model ion channel, resulted in increased membrane conductance. This membrane conductance was diminished when the gramicidin channels were blocked with $CaCl_2$, indicating that the change in membrane conductance results from gramicidin-mediated ion transport. These very stable, biologically functional pore-spanning membranes open many possibilities for silicon-based ion-channel devices for applications such as biosensors and high-throughput drug screening.

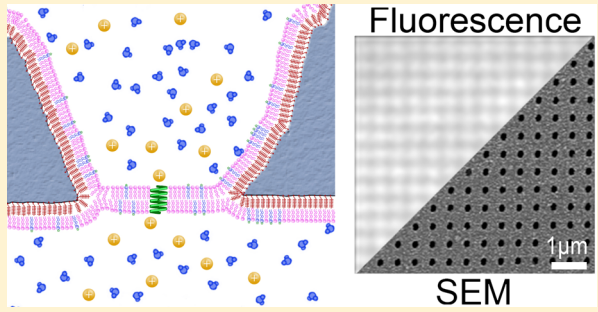

INTRODUCTION

The lipid bilayer membrane serves as the barrier that separates cells from their environment and thus critically regulates material and information flow into biological systems. Because lipid membranes facilitate the highly selective transport of molecules and ions entering and leaving a cell, they have great potential for applications such as drug screening and biological and chemical sensors.[1] Pore-spanning bilayers over micrometer[2−4] and nanoscale[5−17] holes mimic both the nature of in vivo bilayers and their membrane protein's native environment with fluid on both the cis and trans sides. Reducing the pore diameter to nanoscale dimensions improves the stability of the pore-spanning bilayer, a fact that has stimulated the development of substrates with nanoscale pores for lipid membrane studies.[8] Additionally, the creation of arrays of pore-spanning bilayers opens the possibility to use microfluidic automation common with lab-on-a-chip arrangements.[4]

The creation of these pore-spanning membranes has been accomplished by a variety of methods. The application of a lipid solution in an organic solvent (e.g., *n*-decane) across a hole[2,3] or hole array forms a black lipid membrane (BLM).[9,10] A weakness of this approach is that some of the solvent remains in the BLM. The solvent can denature proteins, and as the solvent dissipates, it destabilizes the bilayer and can induce its rupture. A second, solvent-free approach is to deposit the bilayer into place onto the porous surface. Lipid bilayers can be deposited from a cell membrane,[11] from a monolayer-coated bubble,[12] or from a giant unilamellar vesicle (GUV).[13,14] However, these methods do not permit the controlled incorporation of membrane proteins. A more robust way of forming solvent-free pore-spanning bilayers is by the fusion of small unilamellar vesicles (SUVs).[18] These SUVs are capable of the facile incorporation of varied lipid compositions, peptides, and membrane proteins.[19] However, to date, systems using SUVs have achieved limited success in accomplishing high-impedance pore spanning.

Although none of these studies has achieved efficient pore spanning by high-resistance, solvent-free membranes, they have given tremendous insight into the requirements of such a system. First, low surface roughness of the support is necessary to promote bilayer fluidity on the substrate and good sealing at the pore edges while maintaining high impedance across the pores.[15] Second, the surface must be hydrophobic to avoid the formation of an aqueous layer between the bilayer and support, which diminishes the resistance by serving as an ionic reservoir.[16] Finally, Kumar et al. determined that the formation of nanopore-spanning bilayers requires a vesicle diameter larger than the pore diameter to favor pore-spanning bilayers over surface-conforming bilayers.[17]

This Letter describes the combined fluorescence and electrical characterization of pore-spanning, solvent-free lipid membranes formed by the fusion of small (200 nm) vesicles on

Received: December 20, 2012
Revised: March 4, 2013
Published: March 25, 2013

~100 nm diameter nanopores created by e-beam lithography and etched through a freestanding silicon nitride membrane supported on a silicon substrate. By rendering the Si_3N_4 surface hydrophobic using an organosilane layer, we achieve a high electrical resistance (>1 GΩ), which is important for enabling ion current studies. Optically transparent silicon nitride substrates containing an array of 40 000 pore-spanning membranes demonstrate a membrane lifetime in excess of 72 h.

MATERIALS AND METHODS

Device Fabrication. Silicon wafers coated with 200 nm of silicon nitride were patterned and anisotropically etched with KOH to form 100 μm square silicon nitride membranes (Figure 1). A 200 × 200 array of nanopores of ~100 nm diameter and 500 nm pitch was patterned through each membrane using electron-beam lithography and CF_4 plasma etching. A detailed description of the fabrication process is provided in the Supporting Information (SI). Following cleaning, the silicon nitride surface was rendered hydrophobic using an organosilane monolayer formed using either the solution-phase deposition of octadecyltrichlorosilane (OTS, Sigma-Aldrich, MO, USA) or the vapor-phase deposition of tridecafluoro-1,1,2,2-tetrahydrooctyl trichlorosilane (FOTS, Gelest, PA, USA) using a commercial molecular vapor deposition system (AMST MVD100). OTS was deposited on oxygen-plasma-cleaned substrates oriented vertically in a glass beaker to minimize the collection of agglomerates on the silicon nitride surface. Anhydrous toluene was added to the beaker, flushed once, and then replenished. OTS was added to the beaker to make a final dilution of 1:1000 OTS/toluene, and the samples were incubated for 45 min. Following incubation, samples were rinsed twice in toluene, isopropanol, and methanol, respectively, keeping the sample immersed in solvent throughout the process. Finally, substrates were removed and dried in a stream of nitrogen.

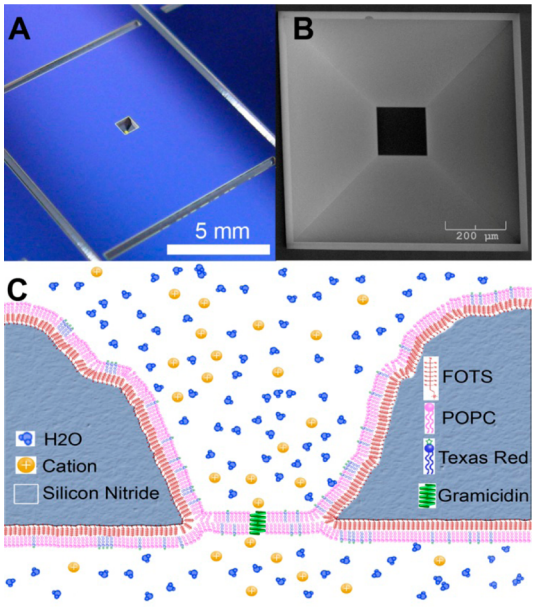

Figure 1. Overview of nanoperforated silicon nitride chips. (A) Photograph of an individual 10 mm × 10 mm silicon chip prior to cleaving. (B) SEM image of a released silicon nitride membrane. (C) Depiction of a nanopore cross-section with a hybrid bilayer on nitride and an ion channel within the pore-spanning bilayer.

Vesicle Fusion and Electrochemical Impedance Spectroscopy (EIS). SUVs were prepared by extrusion (details in Supporting Information). The vesicle solution was diluted 1:1 with 0.1 M sodium phosphate/0.15 M sodium chloride, pH 7 (PBS), and incubated for 5 min over a prewetted porous silicon nitride chip to form pore-spanning bilayers: buffer solution was forcibly introduced from the KOH-etched side of the membrane, and more buffer was then added from the other side to avoid trapping air bubbles during vesicle fusion.

Gramicidin A (Enzo Life Sciences, NY, USA) was used as a model ion channel to demonstrate the biological functionality of the pore-spanning membranes. Gramicidin-containing SUVs were produced by adding 100 ng of gramicidin A to the lipid mixture in chloroform prior to drying, followed by reconstitution and extrusion as described above. If we assume that all of the gramicidin added was incorporated into the lipid bilayer, then the gramicidin/POPC molar ratio was 1:62 000 within the pore-spanning region.

The electrical properties of nanopore chips and lipid membranes on nanopore chips were studied via electrical impedance spectroscopy (EIS). The chip was mounted in a Teflon fixture with 3.68 mm inner-diameter O-rings sealing the top and bottom surfaces of the chip (Supporting Information). The area exposed to buffer solution measured about 11 mm^2. The upper and lower reservoirs are filled with PBS during EIS measurements.

In EIS studies of pore-spanning membranes incorporating gramicidin A, the $CaCl_2$ blocking of gramicidin served as a control to verify that changes in the membrane resistance R_m were due to gramicidin A-mediated ion transport.

Fluorescence Recovery after Photobleaching (FRAP). Subsequent to EIS characterization, the nanoporous chips were transferred underwater from the Teflon EIS cell to a perfusion cell (CoverWell, Invitrogen) for fluorescence imaging to ascertain the fluidity and continuity of the assembled membranes. A detailed description of the fluorescence characterization is found in the Supporting Information.

RESULTS AND DISCUSSION

Nanopore Surface Characterization. We used silicon nitride on silicon wafers because of the ease of adapting standard lithography and etch processes. The fabrication of chips routinely resulted in a 200 × 200 array of nanopores (Figure 1A,B) with a 500 nm pitch (Figure 2A). An inspection of the nanoporous membrane by atomic force microscopy (AFM) using a special slender probe tip with a full cone angle of <10° and a tip radius of <10 nm (Improved Super Cone, ISC75-R, Nanoscience Instruments) reveals a tapered sidewall profile, with the presence of grains sized on the order of 50 nm

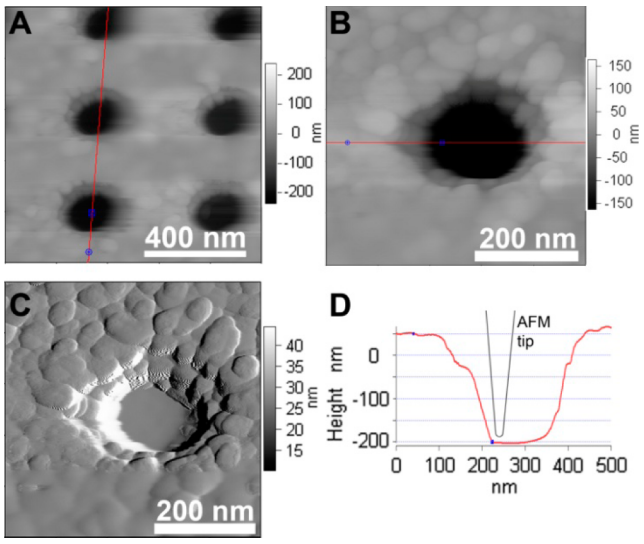

Figure 2. AFM images of a nanopore array. (A) AFM height trace of a subsection of the nitride nanopore array. (B) AFM height trace at higher resolution of an individual nanopore. (C) AFM amplitude trace of the same individual nanopore. (D) AFM line section of an individual nanopore, with an appropriately scaled outline of the special slender probe tip used for imaging.

dx.doi.org/10.1021/la305064j | Langmuir 2013, 29, 4421−4425

and height topography on the order of 20 to 40 nm with smooth transitions between adjacent grains (Figure 2B,C). The nitride surface is relatively smooth and thus well suited to promote bilayer sealing. The diameter of the opening at the bottom of the Si_3N_4 membrane is approximately 130 nm (Figure 2D).

High-Resistance, Fluid Lipid Bilayers Span the Nanopores. Both OTS and FOTS were deposited on silicon nitride membranes to provide surfaces suitable for the formation of a high-resistance bilayer. The vapor-phase FOTS deposition produced extremely clean surfaces, whereas solution-phase OTS deposition initially resulted in contamination resulting from agglomerates arising from ambient humidity. These agglomerates were eliminated by orienting the sample vertically and carefully flushing away the OTS solution as described above.

After exposure to SUVs containing fluorescently labeled lipids, a relatively uniform field of fluorescence is visible on the silicon nitride window (Figure 3). The fluorescence outside the square window is darker, presumably as a result of the destructive interference of the illumination with the strong reflection from the silicon underneath. This effect also seems to reduce the photobleaching of the dye in this region. As a result, the rim of the window appears somewhat brighter because of the diffusion of unbleached dye from beyond it. Inside the square, at high magnification, a regular pattern of uniformly bright spots surrounded by continuous darker regions is visible (Figure 3A, inset). Even though the holes are smaller than the resolving power of the microscope, a pattern of bright spots is still easily discernible because the holes are sufficiently far apart. This pattern is consistent with a single lipid leaflet (a hybrid bilayer) over the nitride surface and two lipid leaflets spanning the holes in the nitride film. The uniformity of the spots suggests that all holes are covered with a lipid membrane. We hypothesize that the pore-spanning membrane forms at the bottom surface of the nitride with a hybrid bilayer on the silicon nitride surface and a full bilayer over the hole, as depicted in Figure 1C.

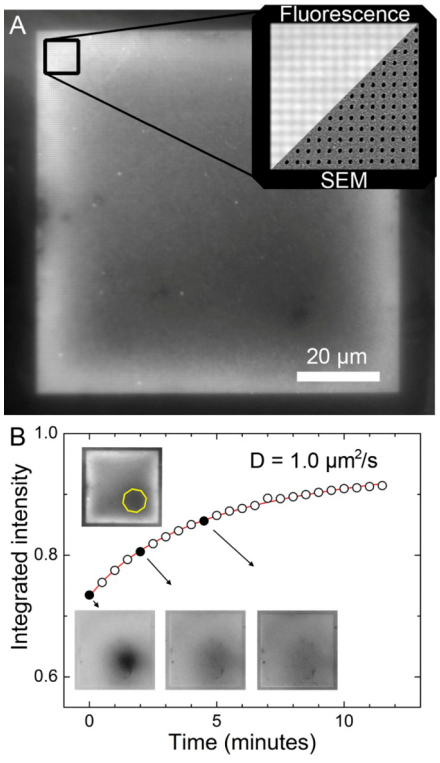

Figure 3. Fluorescence imaging showing a POPC/Texas red–DHPE/FOTS hybrid lipid bilayer across a silicon nitride nanoporous membrane. (A) Image of a 200 × 200 array of 130-nm-diameter holes, showing that a (hybrid) bilayer with good uniformity has formed. The fluorescence outside the 100 μm nitride window is reduced by the reflection from the silicon underneath. (Inset) Magnified view showing the fluorescence of the holes together with a scanning electron micrograph of a gold-sputtered sample. (B) Fluorescence recovery after photobleaching. The top left inset shows the fluorescence before bleaching and the outline of the aperture used. The prebleaching image is divided out from the three frames below that illustrate the recovery.

To characterize the fluidity of the lipids on both FOTS- and OTS-coated substrates, we used FRAP. Figure 3B shows a time-lapse sequence of FRAP images along with a plot of the recovery as a function of time. The fluorophores are already diffusing during the bleaching; the small size of the bleached spot and the reduction in bleaching intensity due to the reflection from the nitride explain the blurring of the initial bleached spot and its modest contrast. A fit to the intensity data yields a diffusion constant of 1.0 ± 0.6 $\mu m^2/s$, which is in good agreement with values observed for POPC hybrid bilayers on silanized glass.[9] We obtained similar diffusion constants for bilayers deposited with either FOTS or OTS.

EIS was used to determine the electrical properties of the lipid film over the nanoporous nitride. An analysis of the EIS time-lapse spectra reveals that at low frequencies (1 mHz < f < 1 Hz) the impedance of the lipid-membrane-coated substrate is dominated by the membrane resistance R_m, which is >1 GΩ. At higher frequencies (1 Hz < f < 10 kHz), the dominant component is the capacitance of the Si_3N_4 layer, C_p. We observe capacitances C_p of 2.5–4.0 nF, which is in excellent agreement with the capacitance expected from the silicon nitride enclosed by the O-ring of 3.5 nF, on the basis of the 11 mm^2 enclosed area, the 200 nm thickness of the nitride, and the dielectric constant ε_r of the nitride of 7.5.

The stability of the pore-spanning membranes was probed by recording the EIS spectra until the observed impedance reached a value close to that of a bare nanopore substrate. EIS spectra collected immediately and 77 and 83 h after vesicle fusion are plotted along with the spectrum of a bare nanopore substrate in Figure 4. The value of R_m extracted from each EIS spectrum is plotted versus time in the inset. The resistance exceeds 3 GΩ up to 71 h. A small decrease in resistance is noticeable at 77 h, followed by a sharp decrease at 83 h. After 129 h of sampling, the bilayer's impedance closely resembles that of the bare substrate. These changes in impedance are consistent with the preparation of well-formed pore-spanning bilayers, persisting for at least 77 h. In some experiments, an intact membrane persists over 140 h.

To assess how sensitive this system is to the rupture of a bilayer over a single pore, we compare the observed resistance change with the expected resistance for a single open hole, based on its geometry and the conductivity of the solution. We estimate the single hole resistance to be 12 MΩ (Supporting Information) and the combined resistance of the 40 000 holes in the membrane to be 0.3 kΩ. This value is lower than the observed low-frequency resistance of a membrane without a bilayer in Figure 4, but this result is attributable to the fact that the resistance of the holes is in series with the impedance of the platinum working electrode. More importantly, the resistance

dx.doi.org/10.1021/la305064j | Langmuir 2013, 29, 4421–4425

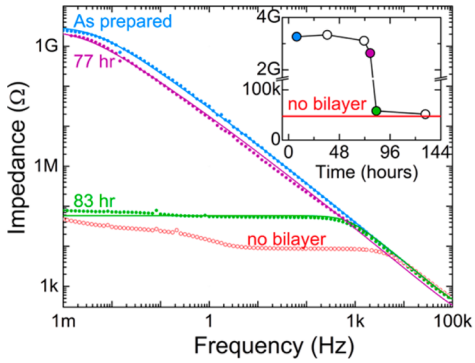

Figure 4. Electrical impedance spectra of a POPC bilayer spanning the 130 nm holes in a perforated silicon nitride membrane, as measured (symbols) and fitted to an equivalent circuit model (curves, Supporting Information). The corresponding membrane resistance is shown in the inset. The membrane shows a gigaohm seal that lasts for several days.

of a bilayer with a single open hole is considerably smaller than the observed gigaohm resistance of a silicon nitride membrane with a bilayer. This fact indicates that the rupture of the bilayer spanning even a single hole is readily noticeable in impedance measurements.

We attribute the observed high degree of coverage of pore-spanning bilayers to the hydrophobic treatment of the relatively smooth nitride membrane, the use of liposomes that are larger than the hole diameter, and the strong curvature of the pore edge. Prewetting the nanoporous nitride membrane before liposome fusion appears to play an important role in this result.

Gramicidin A Is a Functional Ion Channel in Pore-Spanning Membranes. To confirm that these nanoporous supports are suitable as a host for incorporating protein channels, gramicidin A was used as a model ion channel. As shown in Figure 5, the addition of gramicidin lowered the

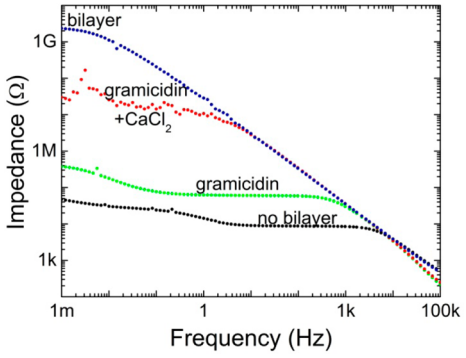

Figure 5. EIS spectra of pore-spanning lipid membranes with and without gramicidin. Adding gramicidin lowers the impedance. Adding calcium chloride (0.1 M) blocks the gramicidin conductance. The low-frequency dispersion at low impedances is attributed to the platinum working electrode; this was confirmed by other measurements (e.g., without the chip in place).

impedance to ∼1 MΩ. On the basis of the relative molar concentrations of gramicidin and POPC and assuming that each lipid molecule occupies an area of 50 Å^2, we expect approximately 43% of the total 40 000 130 nm pore-spanning membranes to contain a gramicidin dimer. Published values for gramicidin conductance[20−22] range from 5 to 80 pS, which would result in a membrane resistance of between 0.3 and 5 MΩ, a range consistent with our experimental measurements.

To confirm that the observed decrease in impedance was due to ion transport through gramicidin pores, we added 100 mM $CaCl_2$, which displays a shielding effect on the gramicidin pores against monovalent cations. The $CaCl_2$ solution increased the membrane resistance to approximately 20 MΩ, roughly 50× greater than the initial resistance. The original impedance was recovered by flushing the cell with PBS, thereby indicating successful biologically functional pore-spanning membranes.

CONCLUSIONS

The combined electrical and fluorescence measurements presented here show that using vesicle fusion is a beneficial route for creating functional solvent-free pore-spanning bilayer membranes. The stability of the pore-spanning bilayers is about 77 h, and on occasion we have observed lifetimes extending over 140 h.

We have successfully created hybrid bilayers using both liquid-phase octadecyl trichlorosilane (OTS) and vapor-phase tridecafluoro-1,1,2,2-tetrahydrooctyl trichlorosilane (FOTS) surface functionalizations. We achieved a reduction in agglomerate formation during the liquid-phase deposition of OTS by careful multiple-step rinsing while keeping the surfaces vertically oriented. Vapor-phase silanization circumvented issues with agglomerates entirely, thereby improving surface quality.

The EIS and FRAP data of the nanopore-spanning bilayers paint a consistent picture, one in which a high impedance or functional bilayer is also a bilayer that has good uniformity and fluidity.

ASSOCIATED CONTENT

Supporting Information

Details of vesicle fusion. Electrochemical impedance spectroscopy. Fluorescence recovery after photobleaching. This material is available free of charge via the Internet at http://pubs.acs.org.

AUTHOR INFORMATION

Corresponding Author

*E-mail: dahorsley@ucdavis.edu.

Notes

The authors declare no competing financial interest.

ACKNOWLEDGMENTS

We thank Frank Yaghmaie and the staff at the UC Davis Northern California Nanotechnology Center for fruitful discussions. We also thank Dawn Hilken for experimental support. Work at the Molecular Foundry was supported by the Office of Science, Office of Basic Energy Sciences of the U.S. Department of Energy under contract no. DE-AC02-05CH11231. Work at UC Davis was supported in part by the Materials Design Institute at UC Davis, which is funded by the Los Alamos National Laboratory/UC Davis Educational Collaborative (subcontract no. 2511-002-06).

REFERENCES

(1) Durick, K.; Negulescu, P. Cellular biosensors for drug discovery. *Biosens. Bioelectron.* **2001**, *16*, 587−592.

(2) Suzuki, H.; Tabata, K. V.; Noji, H.; Takeuchi, S. Electrophysiological recordings of single ion channels in planar lipid bilayers using a polymethyl methacrylate microfluidic chip. *Biosens. Bioelectron.* **2007**, *22*, 1111−1115.

(3) Hirano-Iwata, A.; Aoto, K.; Oshima, A.; Taira, T.; Yamaguchi, R. T.; Kimura, Y.; Niwano, M. Free-standing lipid bilayers in silicon chips-membrane stabilization based on microfabricated apertures with a nanometer-scale smoothness. *Langmuir* **2010**, *26*, 1949−1952.
(4) Zagnoni, M.; Sandison, M. E.; Marius, P.; Lee, A. G.; Morgan, H. Controlled delivery of proteins into bilayer lipid membranes on chip. *Lab Chip* **2007**, *7*, 1176−1183.
(5) Kresak, S.; Hianik, T.; Naumann, R. L. C. Giga-seal solvent-free bilayer lipid membranes: from single nanopores to nanopore arrays. *Soft Matter* **2009**, *5*, 4021−4032.
(6) Drexler, J.; Steinem, C. Pore-suspending lipid bilayers on porous alumina investigated by electrical impedance spectroscopy. *J. Phys. Chem. B* **2003**, *107*, 11245−11254.
(7) Schmitt, E. K.; Nurnabi, M.; Bushby, R. J.; Steinem, C. Electrically insulating pore-suspending membranes on highly ordered porous alumina obtained from vesicle spreading. *Soft Matter* **2008**, *4*, 250−253.
(8) Simon, A.; Girard-Egrot, A.; Sauter, F.; Pudda, C.; D'Hahan, N. P.; Blum, L.; Chatelain, F.; Fuchs, A. Formation and stability of a suspended biomimetic lipid bilayer on silicon submicrometer-sized pores. *J. Colloid Interface Sci.* **2007**, *308*, 337−343.
(9) White, R. J.; Ervin, E. N.; Yang, T.; Chen, X.; Daniel, S.; Cremer, P. S.; White, H. S. Single ion-channel recordings using glass nanopore membranes. *J. Am. Chem. Soc.* **2007**, *129*, 11766−11775.
(10) Han, X. J.; Studer, A.; Sehr, H.; Geissbuhler, I.; Di Berardino, M.; Winkler, F. K.; Tiefenauer, L. X. Nanopore arrays for stable and functional free-standing lipid bilayers. *Adv. Mater.* **2007**, *19*, 4466−4470.
(11) Danelon, C.; Perez, J. B.; Santschi, C.; Brugger, J.; Vogel, H. Cell membranes suspended across nanoaperture arrays. *Langmuir* **2006**, *22*, 22−25.
(12) Mager, M. D.; Melosh, N. A. Nanopore-spanning lipid bilayers for controlled chemical release. *Adv. Mater.* **2008**, *20*, 4423−4427.
(13) Lazzara, T. D.; Kliesch, T. T.; Janshoff, A.; Steinem, C. Orthogonal functionalization of nanoporous substrates: control of 3D surface functionality. *ACS Appl. Mater. Interfaces* **2011**, *3*, 1068−1076.
(14) Mey, I.; Steinem, C.; Janshoff, A. Biomimetic functionalization of porous substrates: towards model systems for cellular membranes. *J. Mater. Chem.* **2012**, *22*, 19348−19356.
(15) Hennesthal, C.; Drexler, J.; Steinem, C. Membrane-suspended nanocompartments based on ordered pores in alumina. *ChemPhysChem* **2002**, *3*, 885−889.
(16) White, R. J.; Zhang, B.; Daniel, S.; Tang, J. M.; Ervin, E. N.; Cremer, P. S.; White, H. S. Ionic conductivity of the aqueous layer separating a lipid bilayer membrane and a glass support. *Langmuir* **2006**, *22*, 10777−10783.
(17) Kumar, K.; Isa, L.; Egner, A.; Schmidt, R.; Textor, M.; Reimhult, E. Formation of nanopore-spanning lipid bilayers through liposome fusion. *Langmuir* **2011**, *27*, 10920−10928.
(18) Cremer, P. S.; Boxer, S. G. Formation and spreading of lipid bilayers on planar glass supports. *J. Phys. Chem. B* **1999**, *103*, 2554−2559.
(19) Doeven, M. K.; Folgering, J. H. A.; Krasnikov, V.; Geertsma, E. R.; van den Bogaart, G.; Poolman, B. Distribution, lateral mobility and function of membrane proteins incorporated into giant unilamellar vesicles. *Biophys. J.* **2005**, *88*, 1134−1142.
(20) Wallace, B. A. Gramicidin channels and pores. *Annu. Rev. Biophys. Bio.* **1990**, *19*, 127−157.
(21) Bamberg, E.; Lauger, P. Blocking of gramicidin channel by divalent-cations. *J. Membr. Biol.* **1977**, *35*, 351−375.
(22) Gambale, F.; Menini, A.; Rauch, G. Effects of calcium on the gramicidin-A single channel in phosphatidylserine membranes - screening and blocking. *Eur. Biophys. J.* **1987**, *14*, 369−374.